

CHARACTERIZATION AND MODELLING OF PROPAGATION EFFECTS IN 20-50 GHz BAND

D. Vanhoenacker-Janvier⁽¹⁾, C. J. Gibbins⁽²⁾, C. J. Walden⁽²⁾, C. L. Wrench⁽²⁾, S. Ventouras⁽²⁾, J. Spiegel⁽¹⁾, C. Oestges⁽¹⁾, D. Mertens⁽¹⁾, A. Martellucci⁽³⁾

⁽¹⁾*Microwave Laboratory, UCL, Place du Levant, 3, B1348 Louvain-la-Neuve, Belgium*

⁽²⁾*RCRU, CCLRC-Rutherford Appleton Laboratory, Chilton, Didcot, OX11 0QX, UK*

⁽³⁾*TOS-EEP, ESA, ESTEC, Keplerlaan 1, PB 299, NL-2200 AG Noordwijk, The Netherlands*

INTRODUCTION

With the rapid expansion in demand for new and global broadband communications services comes the need to develop higher frequency bands. Such services can only be provided on a truly global basis by satellite systems, and new architectures for such satellite-based communications rely on the full exploitation of the 20/30 and 40/50 GHz frequency bands. The evolution towards global scales of delivery brings with it a requirement for innovative services to be provided in a consistent way to all regions of the world. It therefore becomes necessary to consider, in the design of new systems, geographic regions which were not hitherto taken in account by regional operators. The exploitation of the higher frequency bands introduces new problems in system design, in particular the accurate determination of link budgets. Propagation through the Earth's atmosphere has a major impact on system design, and the various propagation effects, such as attenuation and scintillation, increase in importance compared with lower frequency bands, requiring a high degree of accuracy and comprehensiveness in their prediction, to encompass all possible propagation impairments, the results of which can be critical in the assessment of system feasibility.

New models are being developed, in the frame of an ESA contract. A model for rain attenuation is developed, based on the full rainrate distribution rather than on the rainrate exceeded at a particular time percentage. Furthermore, new specific attenuation coefficients k and α have recently been developed, which should lead to better accuracy in the 20-50 GHz frequency band. Models for cloud attenuation, scintillation and depolarisation are presented in this paper.

CLOUD ATTENUATION

In this work we present a method to predict cloud attenuation statistics from available liquid water path (LWP) statistics taking into account the cloud temperature. The method is based on the ECMWF ERA40 database of liquid water content and air temperature profiles.

Cloud attenuation is a significant attenuation factor for signals traversing the atmosphere at frequencies above 20GHz. Clouds consist of particles of water in the liquid or ice phase. The proportion of liquid water and ice particles depends on the cloud type. The attenuation due to ice particles can be neglected in the microwave frequency range, and ice particles contribute only to signal depolarisation. Since the sizes of cloud particles are very small in comparison to wave length, the Rayleigh approximation of Mie scattering theory can be used. The specific cloud attenuation is given by [1]:

$$\gamma_c = K_l(f, T) \cdot w \quad [\text{dB/km}] \quad (1)$$

where $K_l(f, T)$ is the specific attenuation coefficient [(dB/km)/(g/m³)], which depends on the cloud temperature T and the signal frequency f . The integrated cloud attenuation on a vertical path is:

$$A = \sum \gamma_{ci} \cdot \Delta l_i = \sum K_l(f, T_i) \cdot w_i \cdot \Delta l_i \quad [\text{dB}] \quad (2)$$

where $K_l(f, T_i)$, T_i , w_i are the vertical profiles of the specific attenuation coefficient, cloud temperature and liquid water density respectively. Δl_i [km] is the differential increment of altitude.

Study of the specific attenuation (as estimated using the liquid water density values and the corresponding cloud temperature values from ERA40 database) versus the liquid water density suggests that we should consider the specific attenuation :

$$\gamma_{ci} = K_l(f, T_f) \cdot w_i + \varepsilon_i \quad (3)$$

where T_f is an effective cloud temperature and ε_i a random error due to cloud temperature spread for the same liquid water density values. Applying equation (3) to equation (2) we have for the integrated attenuation:

$$A = 10^{-3} \cdot K_l(f, T_f) \cdot L + \varepsilon \quad (4)$$

where

$$L = \sum w_i \cdot \Delta l_i \quad [\text{g/m}^2] \quad (5)$$

is the LWP and $\varepsilon = \sum \varepsilon_i \cdot \Delta l_i$.

The effective cloud temperature T_f of model (4) has been estimated by applying weighted least square regression to ECMWF data for Chilbolton-UK, Pomezia-Italy, and Singapore over the period January '00 to December'00. The characteristics of the effective temperature were studied for the frequency range 20 GHz to 50 GHz.

The derived conclusions are:

- a) It seems that LWP statistics can be easily converted to cloud attenuation statistics using $\hat{A} = 10^{-3} \cdot K_l(f, T_f) \cdot L$.
- b) The effective temperature seems to be dependent on the location and practically independent of frequency. Fig. 1 shows the practical independence between the effective temperature and the frequency in an engineering way. For the dataset of 50 GHz we plot the estimated attenuation $\hat{A} = 10^{-3} \cdot K_l(f, T_f) \cdot L$ using the effective temperature derived from the above regression method for this frequency (red line). This is then compared with what results from using an 'inappropriate' effective temperature (blue line), i.e. that derived from the same LWP data but for 20 GHz. Analysis of more years of data will show the potential dependence of effective temperature on seasons.

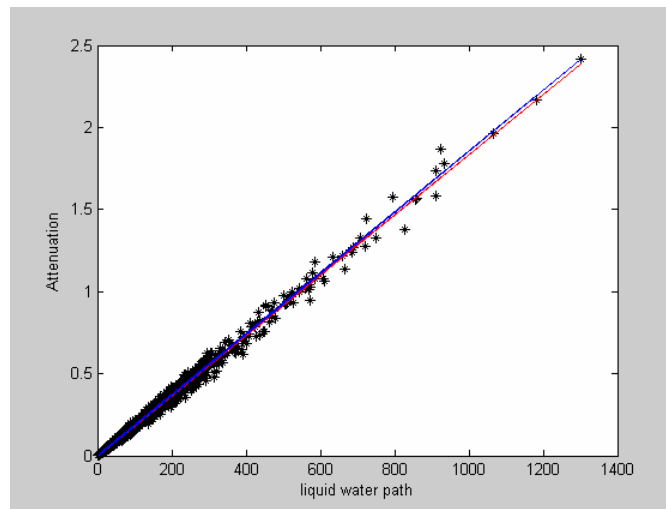


Fig. 1: Comparison of the fitted lines using different effective temperature values as estimated over the period Jan'00-Dec'00 for Chilbolton at 50 GHz (red line) and 20 GHz (blue line). **Black asterisks:** Integrated Attenuation versus Liquid Water Path over the period Jan'00- Dec'00. Chilbolton at 50GHz

RAIN DEPOLARISATION

The full characterization of a depolarizing medium relies on the estimation of the transfer matrix, which is a 2 x 2 matrix relating the actual electric field vector with the vector which would be obtained in the absence of the atmospheric phenomena. If all polarization parameters are to be considered, a complete stochastic model can be obtained using the so-called "quasi-physical" parameters (anisotropy and canting angle). These parameters are strictly related to the physical mechanisms producing depolarization (hydrometeor axes, turbulence, etc.) and can be predicted from climatic parameters [2][3][4].

The procedure removes all clear-sky drifts and variations on the co- and crosspolar signals, thanks to an "almost-automatic" procedure (for long-term analysis); the template is thus estimated by means of a combination of methods, but manual corrections are still possible. The separation between rain and ice is based on the differential attenuation (which is caused only by rain) between co and cross-polar signals, and the differential phase shift (resulting from both rain and ice). Based on the respective differential attenuation and phase shifts, the ice crystal concentration and the instantaneous rain rate are extracted. Based on a T-matrix software for the evaluation of the scattering parameters of the rain drops, and the extracted parameters, the rain XPD is reconstructed. The ice XPD is then also. The total XPD is finally estimated based on the assumption of a cascaded medium. The final results are given in Fig. 2. It can be observed that the agreement between measured (black) and estimated (red) XPD values is quite good.

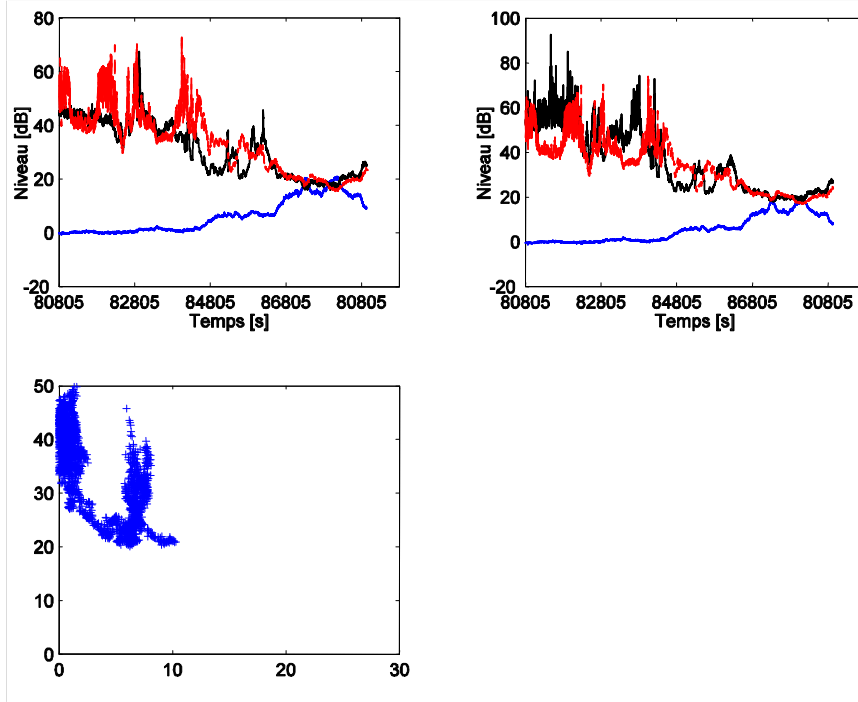


Fig. 2: Comparison between measured and estimated XPD (example at 20 GHz, corresponding to the same event)

SCINTILLATION

Fast fluctuations of received carrier signal-levels on earth-space links, known as amplitude and phase scintillations, are characterised by random successive fades and enhancements associated small-scale refractive-index inhomogeneities within the atmospheric volume intercepted by the Fresnel ellipsoid of microwave links. Above a few GHz, tropospheric turbulence becomes the prevailing source of scintillation, while the contribution of the ionosphere is no more noticed. Amplitude scintillation effects may reduce the effectiveness of beacon-assisted antenna tracking systems and other open-loop fade mitigation techniques.

The aim of the developed software is the creation of a long-term prediction of scintillation statistics under clear-air conditions. The first step is to process the radiosonde data from British Atmospheric Data Centre (BADC), by interpolation so that the data are available at equidistant height intervals of 50 m. The computation of the expected value of C_n^2 is done for each layer. It can be calculated for one or several months, a season or a year. The outputs of the program include the mean of the expected value of C_n^2 , the median and the standard deviation. The scintillation parameters m and s [5] are estimated by taking the frequency, the elevation angle, the antenna efficiency, the physical diameter and the estimated values of C_n^2 . The output parameters allow the prediction of long-term scintillation statistics.

The classical radiosonde profiles (BADC) are used for this software; a single launch is taken. The C_n^2 parameter is calculated for each horizontal layer, starting from an upper altitude of 10 km, using a method similar to the one of Warnock. The variance of the layer is calculated as follows:

$$\sigma_\chi^2 = \int C_n^2 z^{5/6} dz \quad (6)$$

The layer is kept if its contribution to the global variance is significant (above the mean value obtained by the variance divided by the total number of layers) and if $Ri < 0.25$, where Ri is the Richardson number. The Richardson number is the ratio between buoyancy and shear forces and is calculated from the vertical gradients of potential temperature and velocity extracted from the radiosonde data.

The electromagnetic field is calculated, coming from the satellite. The plane wave arrives close to the upper turbulent layer, at 10 km height. The method of phase-screens is used for the evaluation of the field in the turbulent region: it is calculated in blocs whose position and size has to be calculated. The z -coordinate is taken in the direction of the propagation (earth-space direction) and the distance between two phase-screens is taken as $L_0/2$, for L_0 being the outer scale of turbulence for which a conservative value of 100m is taken. The distance may be smaller if the turbulence is intense. Furthermore, each phase screens is correlated with its two neighbours. The x and y coordinates are taken in the plane of calculation. The total dimension in this plane is evaluated, taking into account the total duration of the time series (max 60 sec.), the wind speed and direction, as well as the maximum order of the Fresnel zone used in the simulation. The discretization in x and y coordinates is given by the size of the largest Fresnel zone (2^n for Fourier) and

changes from one plane to the next one. The grid is centred on the link. Inside the surface (x,y), a random generation of the refractive index field, corrected for intermittency, takes place. The spatial correlation is taken into account in the layer and with the two contiguous ones. The layer moves by the wind and the hypothesis of frozen turbulence is taken.

The field is then calculated for each time slot Δt , crossing the phase screen. If the horizontal layer is not considered as turbulent, the classical theory of Huyghens is applied, if the layer is turbulent, the theory of phase screen is applied. Arriving in the plane of the antenna, the field is integrated and the received signal is represented in amplitude and phase. Simulated amplitude scintillation is shown in Fig. 3.

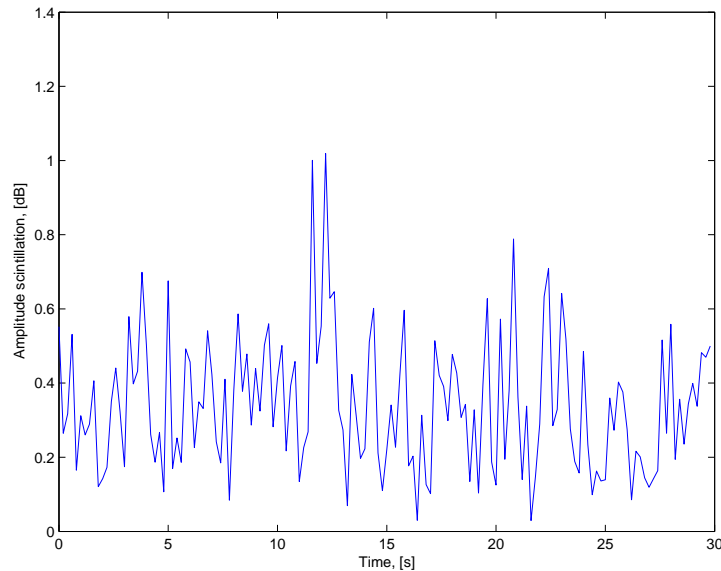


Fig. 3: Simulated scintillation amplitude, at 19 GHz, for an antenna diameter of 1 m and an elevation angle of 83 degrees.

CONCLUSION

New propagation models have been developed in the 20-50 GHz frequency range, keeping in mind the future potential satellite applications. Final results will be presented at the conference, in the field of cloud and rain attenuation, scintillation and depolarisation.

REFERENCES

- [1] H.J. Liebe, "MPM- An Atmospheric Millimeter-Wave Propagation Model", *Int. J. Infrared and Millimeter Waves*, 1989, Vol.10, No. 6,1989, pp 631-650
- [2] Martellucci M. and Paraboni A., "Measurements and modelling of rain and ice depolarization on spatial links in the Ka and V band frequency bands", *Millennium Conference on Antennas and Propagation AP 2000*, on CD-ROM.
- [3] Martellucci A., Poiars Baptista J. P. V. and Blarzino G., "New climatological databases for ice depolarization on satellite radio links", *COST 280 1st International Workshop on Propagation Impairment Mitigation for Millimetre Wave Radio Systems*.
- [4] van de Kamp M. M. J. L., "Climatic radiowave propagation models for the design of satellite communication systems", PhD Thesis, Technical University of Eindhoven, 1999, 226 p.
- [5] ITU-R Recommendation P.618-8, "Propagation data and prediction methods required for the design of Earth-space telecommunication systems", Recommendations of the ITU, International Telecommunications Union, ITU-R, 2003.